International Journal of Advanced Mechanical Engineering.
ISSN 2250-3234 Volume 6, Number 1 (2016), pp. 1-15

http://www.ripublication.com

Application of modified couple stress theory to study dynamic characteristics of electrostatically actuated micro-beams resting upon squeeze-film damping under mechanical shock

Emran Khoshrouye Ghiasi

Master of Science, Department of Mechanical Engineering,
Ferdowsi University of Mashhad, Mashhad, Iran
em.khoshrou@alumni.um.ac.ir

Abstract

In this paper, the dynamic characteristics of clamped-clamped silicon micro-beam subjected to electrostatic excitation and mechanical shock is investigated. The Euler-Bernoulli beam model based on the modified couple stress theory with von Kármán geometric non-linearity is utilized in theoretical formulation. Afterwards, squeeze-film damping effects of micro-structures for small amplitude vibration are analyzed through Reynolds equation. In this regard, the generalized differential quadrature method is used to solve dimensionless governing equations of micro-beam numerically. Overall, it is shown that the pull-in phenomena in electrically actuated MEMS is size dependent. There are also a relation between pull-in voltage and dimensionless mid-point deflection.

Keywords: Micro-beam, Modified couple stress theory (MCST), Squeeze-film damping (SQFD), Pull-in, Mid-point deflection.

1. Introduction

As for an outstanding achievements of micro-machined technology, microelectromechanical systems (MEMS) are extensively utilized in different fields such as automotive industry, resonant sensors, medical, radio frequency (RF) switches, and consumer electronics [1, 2, 3, 4]. At the present moment, it is perfectly possible to produce effective and low cost MEMS with movable parts that range in size from 0.1 to 100 microns, require little power, and operate at high speed [5]. Thus,

these structures are fundamentally made up plates, beams, membranes, or some combined arrangements of such simple structural elements.

In electrostatically actuated MEMS, it is important to note that mechanical and electrostatic forces are essentially coupled [6]. Besides, precise modeling the electrostatic micro-structures is a formidable challenge in view of the mechanical-electrical coupling effects and the non-linearity of the system [3]. To clarify, a paper [7] provided a modeling MEMS resonators past pull-in including a non-linear foundation of springs and dampers between the beam and substrate. In general, the closed-form solution to solve such problems is not available because of highly complex non-linear nature. For instance, Wang et al. [8] studied characterization of extensional multi-layer micro-beams in the presence of pull-in phenomenon and vibrations.

One of the most important phenomena connected with the MEMS concept is pull-in instability, which is discontinuously associated with the interaction of the elastic and electrostatic forces [9, 10]. In other words, the pull-in instability led to limit range of stable equilibrium states of the oscillatory system, and in fact, limits the performance of the actuator [11]. Recently, numerous experimental and numerical studies have been dedicated on the pull-in instability of MEMS. Mojahedi et al. [12] proposed static pull-in analysis of electrostatically actuated micro-beams using homotopy perturbation method, to obtain influence of mid-plane stretching, axial loading, and electrostatic actuation on the system. Hu et al. [13] studied pull-in analysis of electrostatically actuated curved micro-beams with large deformation as well. Subsequently, Size-dependent dynamic pull-in instability of vibrating electrically actuated micro-beams based on the strain gradient elasticity theory has been presented by Sedighi [14]. This survey indicated that by increasing the actuation voltage parameter, the stable center point loses its stability and coalesces with unstable saddle node. In order to account the high-frequency actuation, Lakrad and Belhaq [15] investigated suppression of pull-in instability in MEMS induced by a DC tension. The main result of this paper demonstrated that it is possible to suppress the electrostatically induced pull-in instability for a wide range of the amplitude and frequency.

The strong motivations of investigating damping in MEMS are linked to the connection of energy dissipations with the dynamic response and final specifications of the device [16]. To this end, squeeze-film damping (SQFD) happens because of the massive movement of the fluid underneath the plate, which is assumed to be resisted by the viscosity of fluid [17]. Regarding to this subject, Keyvani et al. [80] investigated effects of squeeze-film damping on a clamped-clamped beam MEMS filter based on modal Galerkin reduced order method, step by step linearization and state space formulation. Li et al. [18] proposed a numerical molecular dynamics approach for squeeze-film damping of perforated MEMS structures in the free molecular regime. Typically, Squeeze-film damping can be modeled using Reynolds equation [19], which is derived from the Navier-Stokes and continuity equations. Bao et al. [20] developed modified Reynolds equation and analytical analysis of squeeze-film air damping of perforated structures. Their results showed that for a rectangular plate with comparable dimensions in the two directions, a solution to the modified

Reynolds equation has been found in series form. Meanwhile, Liu and Wang [21] used squeeze-film damping effects to study non-linear dynamic behavior of electrically-actuated clamped-clamped micro-beam numerically.

Totally, to enhance the efficiency of micro-structures in the presence of pull-in instability and squeeze-film damping, different strategies can be employed. In this case, vibrational analysis of electrostatically actuated micro-structures considering non-linear effects should be attributed to Moghimi Zand and Ahmadian [22], whose work predicted response frequencies of micro-plates based on first-order shear deformation theory (FSDT). Also, by applying finite-difference technique, Bellardineli et al. [23] studied static and dynamic behavior of MEMS subjected to thermoelastic and squeeze-film effects. Abtahi et al. [24] investigated effects of the van der Waals (vdW) force, squeeze-film damping effects, and constant bounce on the dynamics of electrostatic micro-cantilevers before and after pull-in. They approximated applied voltage and beam deflection in the presence of surface adhesion using the Hamilton's principle.

In what follows, dynamic characteristics of electrostatically actuated micro-beams resting on squeeze-film damping under mechanical shock are investigated. First, it will be shown that modified couple stress theory (MCST) contains only one material length scale parameter and is related to both strain and curvature tensors. Then, by employing the electrostatic force, the Euler-Bernoulli theory (EBT), Reynolds equation, and shock force, the dimensionless governing equations of the clamped-clamped micro-beam are derived and the numerical solutions are presented based on the generalized differential quadrature method (GDQM). Finally, the effects of the applied voltage, pressure, and dynamic load on the pull-in instability of the system are examined.

2. Overview of modified couple stress theory

According to the modified couple stress theory [25], the strain energy density is written as

$$\tilde{U} = \frac{1}{2}\int_{\Omega} \sigma_{ij}\varepsilon_{ij} + m_{ij}\chi_{ij}\ dV, \qquad i, j = 1,2,3 \tag{1}$$

where σ, ε, m, and χ are the stress tensor, classical strain tensor, deviatoric part of the couple stress tensor, and symmetric curvature tensor, respectively, defined by

$$\sigma_{ij} = \lambda\ z\ \ \varepsilon_{kk}\delta_{ij} + 2\mu\ z\ \ \varepsilon_{ij}, \tag{2}$$

$$\varepsilon_{ij} = \frac{1}{2}\left(u_{i,j} + u_{j,i}\right), \tag{3}$$

$$m_{ij} = 2\mu\ z\ \left[l\ \ z\ \right]^2 \chi_{ij}, \tag{4}$$

$$\chi_{ij} = \frac{1}{2}\left(\theta_{i,j} + \theta_{j,i}\right), \tag{5}$$

in which δ_{ij}, u_i, and l are the Kronecker delta, components of the displacement vector, and material length scale parameter which reflects the effect of couple stress, respectively, λ and μ are Láme's constants, and θ_i is the components of the rotation vector given as

$$\theta_i = \frac{1}{2} e_{ijk} u_{k,j}, \tag{6}$$

where e_{ijk} is the permutation symbol. It is conceptually useful to regard both σ_{ij} and m_{ij}, as respectively defined in Equations (2) and (4) are symmetric due to the symmetry of ε_{ij} and χ_{ij} given in Equations (3) and (5), respectively.

3. Methodology

3.1. Theoretical background

The purpose of present section is to derive the non-linear governing equations for the micro-beam, by considering the effects of mechanical shock and applied load, geometry, electrostatic excitation, and fluid dynamic behavior. Figure 1 implies a typical clamped-clamped micro-beam which consists of a movable electrode suspended above a fixed ground plate with length *L*, width *b*, and thickness *h*. Moreover, the air initial gap is *d* and an electrostatic force which comes from actuation voltage *V* causes the micro-beam to deflect. All analyses start with the subsequent assumptions for this micro-beam: (i) designating electrostatic excitation by polarized DC voltage, (ii) deduction of equation of motion of micro-beam using Hamilton's principle, (iii) introducing a squeeze-film damping model and associated Reynolds equation, (iv) explanation of mechanical shock, (v) statement of the non-dimensional governing equations due to simplify the numerical simulations, and (vi) Employing different numerical methods to solve the aforementioned dimensionless equations.

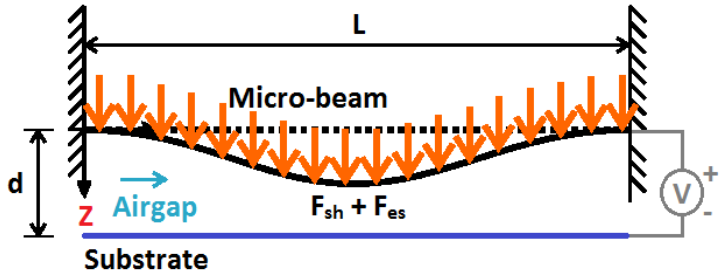

Figure 1. A schematic view of an electrostatically actuated clamped-clamped micro-beam.

3.1.1. Electrostatic excitation

The electrostatic force per unit length acting on such a structure can be written as [26]

$$F_{es} = \frac{\varepsilon b V^2}{2\,(1 - w(x,t))^2}, \tag{7}$$

in which $\varepsilon = 8.854187817620 \times 10^{-12}$ F/m is the vacuum permittivity.

3.1.2. Euler-Bernoulli beam theory

The equation of motion of micro-beam based on the Euler-Bernoulli theory is given by [27]

$$\rho A \frac{\partial^2 w\ \ x,t}{\partial t^2} + EI \frac{\partial^4 w\ \ x,t}{\partial x^4} + p\ \ x,t\ \ b = F_{es} + EA \left[\int_0^L \left(\frac{\partial w\ \ x,t}{\partial x} \right)^2 dx + N_0 \right] \frac{\partial^2 w\ \ x,t}{\partial x^2}, \tag{8}$$

where ρ, A, EI, $p(x,t)$, and N_0 denote the density, area, flexural rigidity, pressure, and applied axial load, respectively. It should be noted that the term $EA \int_0^L \left(\frac{\partial w(x,t)}{\partial x}\right)^2 \mathrm{d}x \frac{\partial^2 w(x,t)}{\partial x^2}$ in above Equation describes the non-linear deflection-dependent stretching of the micro-beam. In actual situation, $p(x,t)$ consists of both ambient pressure P_a and deviatory pressure p. For a clamped-clamped micro-beam, the boundary conditions are considered as follows

$$w\ \ 0,t\ \ = w\ \ L,t\ \ = \frac{\partial w\ \ 0,t}{\partial x} = \frac{\partial w\ \ L,t}{\partial x} = 0. \tag{9}$$

3.1.3. Squeeze-film damping model

When the fluid flow is governed by the continuity and the Navier Stokes momentum equations in continuum regime, it can be validated for unsteady, compressible and viscous flow. In which case, the pressure distribution for the fluid (in particular air) can be found from isothermal non-linear Reynolds equation as follows [19, 28, 21, 29]: (i) the pressure gradient through the air gap is next to zero, (ii) the fluid is Newtonian, (iii) width of the gap separating two plates, whereas the gas is trapped inside, is extensively small compared to the lateral extent of the plates, (iv) the fluid obeys the ideal gas law, and (v) No external forces act on the film.

Therefore, the non-linear Reynolds equation is [29]

$$\nabla . \left(\frac{ph^3}{12\mu} \nabla p \right) = \frac{\partial}{\partial t}\ \ ph\ \ , \tag{10}$$

where μ, ∇p, and h are the fluid viscosity, the gradient of the pressure, and the thickness of the film, respectively. The pressure boundary conditions for the case shown in Figure 1 are as follows

$$\frac{\partial p(0,t)}{\partial x} = \frac{\partial p(L,t)}{\partial x}. \tag{11}$$

3.1.4. Mechanical shock

To illustrate the basic concept of the shock, one may consider as follows

$$F_{sh} = \rho bh \lambda Q\ \ t\ \ , \tag{12}$$

where λ is the amplitude. Now, it is of particular interest to indicate that a shock can be defined as a force applied abruptly and thus in practice, it can be characterized by

maximum value, duration and shape [30]. In other words, the shock forces could be presumed as the superposition of a series of simple shock forces [31]. In this respect, the half-sine shock profile can be expressed mathematically as

$$Q(t)=\sin\left(\frac{\pi t}{\tilde{T}}\right)\underline{U}\ \ t\ \ +\sin\left(\frac{\pi}{\tilde{T}}\ t-\tilde{T}\ \right)\underline{U}\ \ t-\tilde{T}\ \ , \tag{13}$$

in which $T\square$ and $U\square(t)$ are the duration shock and unit step function, respectively.

3.1.5. Dimensionless governing equations of clamped-clamped micro-beam

For analytical convenience, the following dimensionless parameters are introduced as

$$W=\frac{w}{d_0},\ \ X=\frac{x}{L},\ \ T=\frac{t}{\tau},\ \ P=\frac{p}{P_a},\ \ H=\frac{d}{d_0}, \tag{14}$$

where $d_0 = d + w$ and

$$\tau=\sqrt{\frac{\rho AL^4}{EI}}. \tag{15}$$

Substituting the dimensionless parameters given in Equation (14) into Equations (8) and (10), the dimensionless governing equations of clamped-clamped micro-beam under squeeze-film damping and mechanical shock are obtained as

$$\frac{\partial^2 W\ \ X,T}{\partial T^{\ 2}}+\frac{\partial^4 W\ \ X,T}{\partial X^{\ 4}}-\left[\alpha_1\int_0^L\left(\frac{\partial W\ \ X,T}{\partial X}\right)^2 dX\ +N\right]\frac{\partial^2 W\ \ X,T}{\partial X^{\ 2}}$$
$$+\alpha_2 P\ \ X,T\ \ =\alpha_3\frac{V^{\ 2}}{1-W\ \ X,T\ \ ^2}+\alpha_4\bar{Q}\ \ T\ \ , \tag{16}$$

$$\frac{\partial^2 P\ \ X,T}{\partial X^{\ 2}}=\alpha_5\left(\frac{\partial P\ \ X,T}{\partial T}+\frac{\partial H}{\partial T}\right), \tag{17}$$

where the non-dimensional parameters of the system are introduced as

$$\alpha_1=6\left(\frac{h}{d_0}\right)^2,\ \ \alpha_2=\frac{P_a bL^4}{EId_0},\ \ \alpha_3=6\frac{\varepsilon L^4}{Ed_0^2h^3},\ \ \alpha_4=12\frac{\rho\lambda L^4}{Edh^2},\ \ \alpha_5=12\frac{\mu}{P_a d_0^2}\sqrt{\frac{\rho bh}{EI}},\ \ N=N_0\frac{L^2}{EI}. \tag{18}$$

Herein, the non-dimensional shock profile is obtained as

$$Q(T)=\sin\left(\frac{\pi T}{\tilde{T}_n}\right)\underline{U}\ \ T\ \ +\sin\left(\frac{\pi}{\tilde{T}_n}\ T-\tilde{T}_n\ \right)\underline{U}\ \ T-\tilde{T}_n\ \ , \tag{19}$$

where $T\square_n$ is non-dimensional shock duration.

Plus, the non-dimensional boundary conditions are

$$W\ \ 0,T\ \ =W\ \ L,T\ \ =\frac{\partial W\ \ 0,T}{\partial X}=\frac{\partial W\ \ L,T}{\partial X}, \tag{20}$$

$$\frac{\partial P\ \ 0,T}{\partial X}=\frac{\partial P\ \ L,T}{\partial X}=0. \tag{21}$$

3.2. Mathematical solution method

Apart from the sections explained above, in many cases, it may not be possible to solve such non-linear coupled governing equations analytically. As a matter of fact, an approximate solution based on numerical methods will be developed in the following.

3.2.1. Preliminaries

The generalized differential quadrature method was developed by Shu and Richard [32, 33] to modify the differential quadrature method (DQM) for the calculation of weighting coefficients. In this case, one of the best options for taking the grid points is zeros of the well-known Chebyshev-Gauss-Lobatto [33] nodal distribution which ensures the solution procedure and is given as

$$x\ \ i\ \ =\frac{1}{2}\left[1-\cos\left(\pi\frac{i-1}{N\ -1}\right)\right],\quad i=1,2,...,N \tag{22}$$

The first and second order derivatives of an unknown function $f(x,t)$ at a point $x = x_i$ along any line $y = y_j$ parallel to the x-axis, can be approximated by the generalized differential quadrature method as [376]

$$\frac{\partial f}{\partial x}\Big|_{x=x_i}=\sum_{k=1}^{N}A_{ik}^{\ 1}f\quad x_k,y\quad , \tag{23}$$

$$\frac{\partial^2 f}{\partial x^{\ 2}}\Big|_{x=x_i}=\sum_{k=1}^{N}A_{ik}^{\ 2}f\quad x_k,y\quad , \tag{24}$$

where $A_{ik}^{(1)}$ and $A_{ik}^{(2)}$ are the respective weighting coefficients for the first and second order derivatives, respectively. Similarly, the weighting coefficients can be utilized for higher order derivatives, which is expressed as [34]

$$\frac{\partial^m f}{\partial x^{\ m}}\Big|_{x=x_i}=\sum_{k=1}^{N}A_{ik}^{\ m}f\quad x_k,y\quad . \tag{25}$$

As a general rule, for the first order derivative (i.e., $m = 1$) and also for higher order derivatives, one can use the following relations iteratively [32, 34]

$$A_{ik}^{\ m}=m\left[A_{ii}^{\ m-1}A_{ik}^{\ 1}-\frac{A_{ik}^{\ m-1}}{x_i-x_k}\right],\quad i\neq k \tag{26}$$

$$A_{ii}^{\ m}=-\sum_{\substack{j=1\\ i\neq j}}^{N}A_{ij}^{\ m}\ . \tag{27}$$

Due to an externally applied DC voltage across the micro-beam and substrate, determination of the input voltage is vitally important. Indeed, the static pull-in voltage can be considered as an input voltage, which is fortunately calculated with the experimental results of Hung and Senturia [35] and is taken as V_p = 9.2 volts. Nevertheless, it is noted that electrical part of the system has been solved through an iterative Newton-Raphson algorithm [36]. One of the profits of present approach is this method solves the non-linear governing equations by applying the voltage,

computing the corresponding outlets, and then iterate until the drift from outlets is negligible.

To distinguish between electrostatic and mechanical force, Newmark's integration scheme [37, 38] is utilized as a trade-off mechanism between the time domain and applied load. The objective of this approach is to consider implicit time integration over the several time steps.

Lastly, it is important to mention that the integral $\int_0^L \left(\frac{\partial W(X,T)}{\partial X}\right)^2 \mathrm{d}X$ should be calculated numerically by Newton-Cotes quadrature [39], which is constructed by replacing the integrated with an interpolating polynomial of appropriate degree.

3.2.2. Discretization

Based on the generalized differential quadrature method, the non-linear governing equations will be presented as

$$\ddot{W}_i + \sum_{j=1}^{N} A_{ij}^{4} W_j - \left[N - \alpha_1 \sum_{m=1}^{N} \sum_{n=1}^{N} C_m W_m A_{ij}^{2} W_n \right] \cdot \sum_{j=1}^{N} A_{ij}^{2} W_j + \alpha_2 P\ X,T\ = \alpha_3 \frac{V^2}{1-W_i^{\ 2}} + \alpha_4 \bar{Q}_i, \tag{28}$$

$$H^3 P_a \sum_{j=1}^{N} A_{ij}^{\ 2}\ P_j + 3H^2 P_a \sum_{j=1}^{N} A_{ij} W_j = 12\mu\ P_a \dot{W}_i + H\dot{P}_i\ , \tag{29}$$

where C_m is the weighting coefficient in Newton-Cotes quadrature. In addition, boundary conditions can be rewritten as

$$W\ \ 0,T\ = W\ \ L,T\ = \sum_{j=1}^{N} A_{1j} W_j = \sum_{j=1}^{N} A_{Nj} W_j = 0, \tag{30}$$

$$\sum_{j=1}^{N} A_{1j} P_j = \sum_{j=1}^{N} A_{Nj} P_j = 0. \tag{31}$$

4. Results and Discussion

The following numerical results were obtained on a silicon electrostatically micro-beam described entirely in section 3.1. Note that in performing the analysis, the material and geometry analysis of the micro-beam are assigned the values given in Table 1.

Table 1. Parameter values of clamped-clamped silicon micro-beam.

Symbol	Parameters	Value	Dimension
L	Length	400	μm
b	Width	60	μm
h	Thickness	2	μm
d	Initial gap	2.1	μm
E	Young's modulus	166e9	N/m^2
ρ	Density	2330	Kg/m^3
μ	Viscosity	1.82e-5	N/sm^2

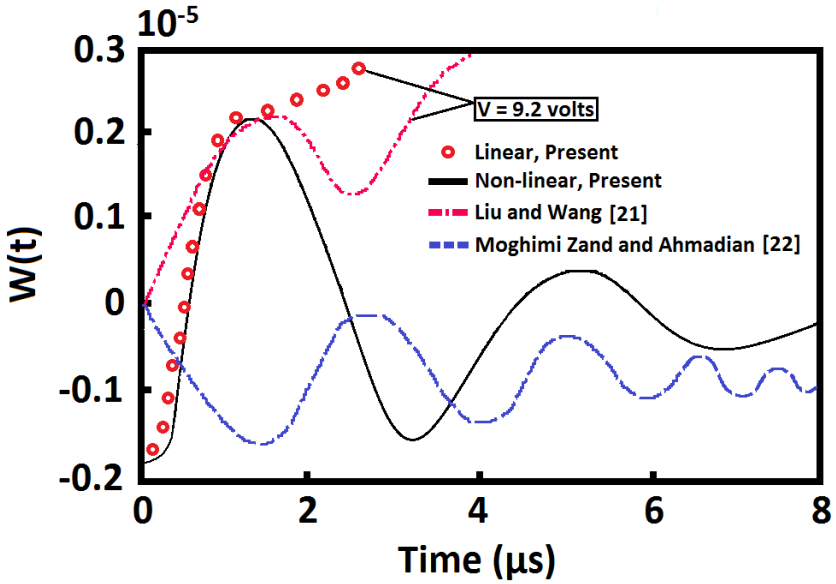

Figure 2. Comparison between the results of present study of dimensionless mid-point deflection vs. time and those reported in [21] and [22].

Figure 2 represents the variation over time of the dimensionless mid-point deflection of the present micro-beam and compares with those reported in [21] and [22]. It is seen that the dimensionless mid-point deflection varies non-linearly due to the electrostatic coupling effects. This figure can also demonstrate that neglecting the non-linear von Kármán strains may lead to estimate linear responses more than non-linear type. It is due to the fact that linear solution of dimensionless governing equations will cause instability before applying voltage. Under the actuation of impose voltage ($V < V_p$), it is clear that results convergences well till t = 2 μs. Nevertheless, for voltage values higher than V_p, there is no static equilibrium in the system [22] and it is likely to encounter with divergence final results. It is noted that the interaction between electrostatic extinction and mechanical shock in the present system can be used for sensing the level of shock acceleration. Furthermore, the micro-beam experiences shock pulse as a static load [381].

Likewise, it is worth noting that Liu and Wang [21] obtained the effect of AC voltage amplitude on the mid-point deflection of the micro-beam and considered different actuating conditions by solving the analytical model using a hybrid numerical scheme. Versus, although Moghimi Zand and Ahmadian [22] multiplied vibrational analysis of micro-structures by solving an eigenvalue problem, we solved the problem without this assumption.

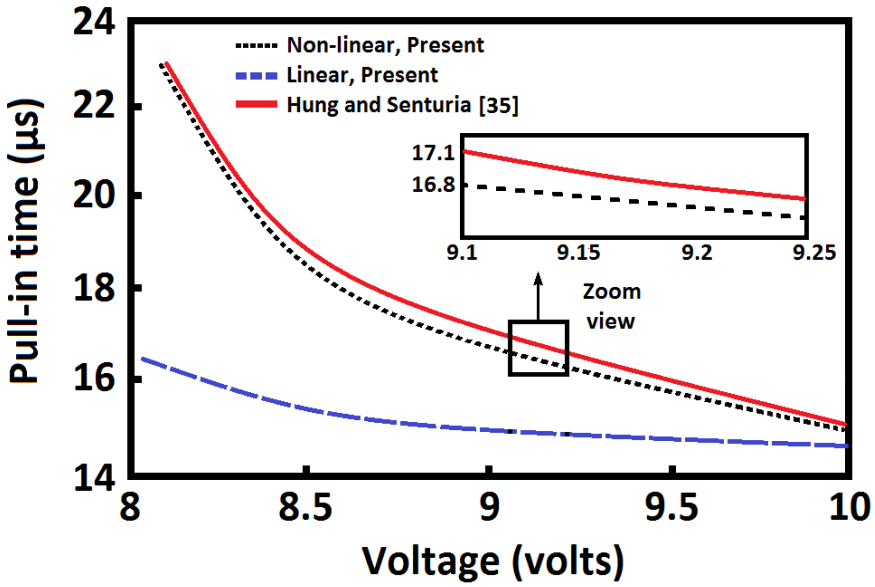

Figure 3. Pull-in time under electrostatic extinction and mechanical shock.

To demonstrate the effect of electrostatic extinction and mechanical shock on the system described by Equation (16), pull-in time response vs. applied voltage are plotted in Figure 3 and have been compared with the obtained experimental results provided by Hung and Senturia [35]. Indeed, the time-varying voltage may induce another type of instability, namely, static pull-in instability due to parametric resonances even for relatively lower voltages. It is to be noted that if the beam thickness is in order of the material length scale, there is a considerable difference between the results of the modified couple stress theory and those evaluated by the others. Based on the results of figure 3, it is found that pull-in time response decreases as the applied voltage increases. In addition, when applied voltage increases, dynamic pull-in instability occurs at lower values of applied voltage.

To go through in details, Figure 3 also shows how the non-linear strain-displacement relations, based on the von-Kármán assumption affect the pull-in characteristics. From this, again, it is demonstrated that although there is a difference between linear and non-linear final results, it is not only dependent on the non-linear strain-displacement relations. On the other hand, this type of dynamic pull-in time increases with increasing the ambient pressure. In this regard, it should be noted that such results are obtained in vacuum pressure ($P_a = 0$).

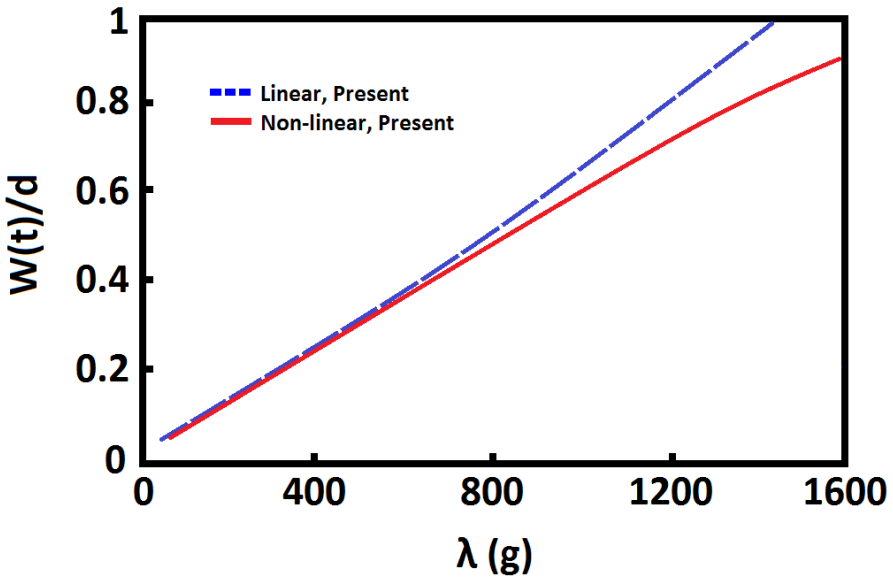

Figure 4. Linear and non-linear ratio of mid-point deflection of micro-beam calculated for T□=1 ms.

Additionally, Figure 4 investigates how the stretching stresses of a silicon micro-beam are influenced by the shock amplitude, where T□=1. Based on the results of this figure, decreasing the shock amplitude parameter leads to a significantly agreement between linear and non-linear findings. This is due to the fact that accounting for couple stress brings about changes non-linearly and (almost) linearly with and without shock amplitude, respectively. As mentioned in such papers [30, 40], the half-sine shock can indicate a good approximation for the shape of actual shock pulse. However, it is also true that for MEMS, the maximum amplitude in shock pulse is larger than the half-sine shock. In this case, more details of Figure 4 are presented in Table 2.

Table 2. Comparison of results of $W(t)/d$ in various shock amplitudes.

λ	Linear	Non-linear	Diversity at each point
0.2	305	311	6
0.4	623	643	20
0.6	920	948	28
0.8	1200	1346	146

Figure 5 emphasizes on the relation between pull-in voltage and dimensionless deflection of the silicon micro-beam. The large difference between the linear and non-linear predictions for maximum pull-in voltage is 25 volts. Moreover, in the case of V

≈ 58 volts and $V \approx 93$ volts, the so-called linear and non-linear dynamic pull-in instability occurs, as plotted in Figure 5. It should be noted that the present discrepancy tends to be much smaller when $d < 2.1$. Overall, such discovery is quite useful for designing efficient MEMS when considering the mechanical loadings.

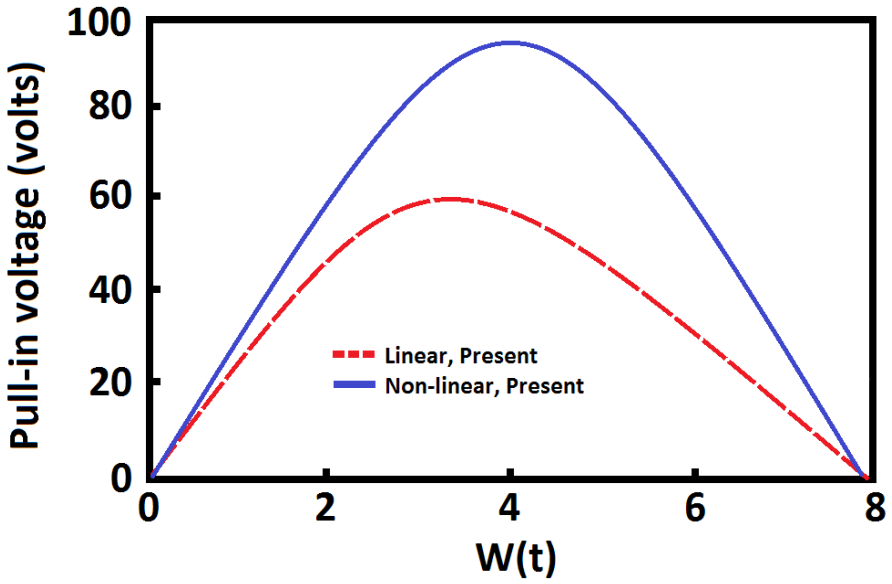

Figure 5. Pull-in voltage vs. *W*(*t*).

5. Conclusion

This letter proposed the use of modified couple stress theory to study dynamic characteristics of electrostatically actuated micro-beams resting on squeeze film damping under mechanical shock. To do so, the silicon micro-beam was considered as a large deflection Euler-Bernoulli beam with von Kármán geometric non-linearity. The generalized differential quadrature method was used as a solution method to numerically solve the dimensionless governing equations and associated boundary conditions. According to the non-linear Reynolds equation and electrostatic extinction, effects of voltage, dynamic loading, and mechanical shock on the response of the system has been studied. In this regard, it was observed that pull-in time varies non-linearly vs. applied voltage. Besides, owing to the early instability in micro-beam through dynamic pull-in, the linear dimensionless mid-point deflection shows higher values than non-linear analysis. Finally, the accuracy of the present iterative approach concurs with available experimental and analytical results published in the literature.

References

[1] He, C.H., Liu, D.C., Zhao, Q.C., En, Y.F., Yang, Z.C, Zhang, D.C. and Yan, G.Z. (2015) A Novel Narrow-Band Force Rebalance Control Method for the Sense Mode of MEMS Vibratory Gyroscopes. *Measurement*, 62, 197-204.

[2] Afrang, S., Mobki, H., Sadeghi, M.H. and Rezazadeh, G. (2015) A New MEMS Based Variable Capacitor with Wide Tunability, High Linearity and Low Actuation Voltage. *Microelectronics Journal*, 46, 191-197.

[3] Chuang, W.C., Lee, H.L., Chang, P.Z. and Hu, Y.C. (2010) Review on the Modeling of Electrostatic MEMS. *Sensors*, 10, 6149-6171.

[4] Ibrahim, M.I., Younis, M.I. and Alsaleem, F. (2010) An Investigation into the Effects of Electrostatic and Squeeze-Film Non-Linearities on the Shock Spectrum of Microstructures. *International Journal of Non-Linear Mechanics*, 45, 756-765.

[5] López, D., Pardo, F., Bolle, C., Decca, R.S. and Bishop, D. (2004) MEMS Technology for the Advancement of Science. *Journal of Low Temperature Physics*, 135, 51-62.

[6] Tilmans, H.A.C. and Legtenberg, R. (1994) Electrostatically Driven Vacuum-Encapsulated Polysilicon Resonators. *Sensors and Actuators*, 45(A), 67-84.

[7] Vyasarayani, C.P., Abdel-Rahman, E.M., McPhee, J. and Birkett, S. (2011) Modeling of Resonators Past Pull-In. *Journal of Computational and Nonlinear Dynamics*, 6, 1-7.

[8] Wang, Y.G., Lin, W.H., Feng, Z.J. and Li, X.M. (2012) Characterization of Extensional Multi-Layer Microbeams in Pull-In Phenomenon and Vibrations. *International Journal of Mechanical Sciences*, 54, 225-233.

[9] Zhang, W.M., Yan, H., Peng, Z.K. and Meng, G. (2014) Electrostatic Pull-In Instability in MEMS/NEMS: A Review. *Sensors and Actuators*, 214(A), 187-218.

[10] Fu, Y. and Zhang, J. (2011) Size-Dependent Pull-In Phenomena in Electrically Actuated Nanobeams Incorporating Surface Energies. *Applied Mathematical Modelling*, 35, 941-951.

[11] Elata, D. and Bamberger, H. (2006) On the Dynamic Pull-In Electrostatic Actuators with Multiple Degrees of Freedom and Multiple Voltage Sources. *Journal of Microelectromechanical Systems*, 15(1), 131-140.

[12] Mojahedi, M., Moghimi Zand, M. and Ahmadian, M.T. (2010) Static Pull-In Analysis of Electrostatically Actuated Microbeams Using Homotopy Perturbation Method. *Applied Mathematical Modelling*, 34, 1032-1041.

[13] Hu, Y.J., Yang, J. and Kitipornchai, S. (2010) Pull-In Analysis of Electrostatically Actuated Curved Micro-beams with Large Deformation. *Smart Materials and Structures*, 19, 1-9.

[14] Sedighi, H.M. (2014) Size-Dependent Dynamic Pull-In Instability of Vibrating Electrically Actuated Microbeams Based on the Strain Gradient Elasticity Theory. *Acta Astronautica*, 95, 111-123.

[15] Lakrad, F. and Belhaq, M. (2010) Suppression of Pull-In Instability in MEMS Using a High-Frequency Actuation. *Commun Nonlinear and Numerical Simulation*, 15, 3640-3646.

[16] De Pasquale, G. and Somà, A. (2015) An Energetic Approach of the Experimental Identification of Damping in Microstructures. *Mechanical Systems and Signal Processing*, 50-51, 338-348.

[17] Nayfeh, A. and Younis, M.I. (2004) A New Approach to the Modeling and Simulation of Flexible Microstructures under the Effect of Squeeze-Film Damping. *Journal of Micromechanics and Microengineering*, 14, 170-181.

[18] Li, P., Fang, Y. and Wu, H. (2014) A Numerical Molecular Dynamics Approach for Squeeze-Film Damping of Perforated MEMS Structures in the Free Molecular Regime. *Journal of Microfluidics and Nanofluidics*, 17, 759-772.

[19] Bao, M. and Yang, H. (2007) Squeeze Film Air Damping in MEMS. *Sensors and Actuators*, 136(A), 3-27.

[20] Bao, M., Yang, H., Sun, Y. and French, P.J. (2003) Modified Reynolds' Equation and Analytical Analysis of Squeeze-Film Air Damping of Perforated Structures. *Journal of Micromechanics and Microengineering*, 13, 795-800.

[21] Liu, C.C. and Wang, C.C. (2014) Numerical Investigation into Nonlinear Dynamic Behavior of Electrically-Actuated Clamped-Clamped Micro-Beam with Squeeze-Film Damping effect. *Applied Mathematical Modelling*, 38, 3269-3280.

[22] Moghimi Zand, M. and Ahmadian, M.T. (2009) Vibrational Analysis of Electrostatically Actuated Microstructures Considering Nonlinear effects. *Commun Nonlinear and Numerical Simulation*, 14, 1664-1678.

[23] Belardinelli, P., Brocchini, M., Demeio, L. and Lenci, S. (2013) Dynamical Characteristics of an Electrically Actuated Microbeam under the Effects of Squeeze-Film and Thermoelastic Damping. *International Journal of Engineering Science*, 69, 16-32.

[24] Abtahi, M., Vossoughi, G. and Meghdari, A. (2014) Effects of the van der Waals Force, Squeeze-Film Damping, and Contact Bounce on the Dynamics of Electrostatic Microcantilevers Before and After Pull-In. *Nonlinear Dynamics*, 77, 87-98.

[25] Yang, F., Chong, A.C.M., Lam, D.C.C. and Tong, P. (2002) Couple Stress Based Strain Gradient Theory for Elasticity. *International Journal of Solids and Structures*, 39, 2731-2743.

[26] Krylov, S. and Seretensky, S. (2006) Higher Order Correction of Electrostatic Pressure and its Influence on the Pull-In Behavior of Microstructures. *Journal of Micromechanics and Microengineering*, 16, 1382-1396.

[27] Nayfeh, A.H. and Pai, P.F. (2004) Linear and Nonlinear Structural Mechanics. Wiley.

[28] Altuğ Bıçak, M.M. and Rao, M.D. (2010) Analytical Modeling of Squeeze Film Damping for Rectangular Elastic Plates Using Green's Functions. *Journal of Sound and Vibration*, 329, 4617-4633.

[29] Blech, J.J. (1983) On Isothermal Squeeze Films. *Journal of Lubrication Technology*, 105, 615-620.

[30] Fathalilou, M., Motallebi, A., Yagubizade, H., Rezazadeh, G., Shirazi, K. and Alizadeh, Y. (2009) Mechanical Behavior of an Electrostatically-Actuated Microbeam under Mechanical Shock. *Journal of Solid Mechanics*, 1, 45-57.

[31] Fang, X.W., Huang, Q.A. and Tang, J.Y. (2004) Modeling of MEMS Reliability in Shock Environments. 7*th International Conference on Solid-State and Integrated Circuits Technology*, 860-863.

[32] Shu, C. and Richards, B.E. (1992) Parallel Simulation of Incompressible Viscous Flows by Generalized Differential Quadrature. *Computing Systems in Engineering*, 3, 271-281.

[33] Shu, C. and Richards, B.E. (1992) Application of Generalized Differential Quadrature to Solve Two-Dimensional Incompressible Navier-Stokes Equations. *International Journal for Numerical Methods in Fluids*, 15, 791-798.

[34] Bellman, R., Kashef, B.G. and Casti, J. (1972) Differential Quadrature: A Technique for the Rapid Solution of Nonlinear Partial Differential Equations. *Journal of Computational Physics*, 10, 40-52.

[35] Hung, E.S. and Senturia, S.D. (1999) Generating Efficient Dynamical Models for Microelectromechanical Systems from a Few Finite-Element Simulation Runs. *Journal of Microelectromechanical Systems*, 8(3), 280-289.

[36] Sheng, D., Sloan, S.W. and Abbo, A.J. (2002) An Automatic Newton-Raphson Scheme. *The International Journal of Geomechanics*, 2(4), 471-502.

[37] Rubin, M.B. (2007) A Simplified Implicit Newmark Integration Scheme for Finite Rotations. *Computers and Mathematics with Applications*, 53, 219-231.

[38] Artuzi, W. (2005) Improving the Newmark Time Integration Scheme in Finite Element Time Domain Methods. *Microwave and Wireless Components Letters*, 15(12), 2005.

[39] Burg, C.O.E. (2012) Derivative-Based Closed Newton-Cotes Numerical Quadrature. *Applied Mathematics and Computation*, 218, 7052-7065.

[40] Askari, A.R. and Tahani, M. (2014) An Alternative Reduced Order Model for Electrically Actuated Micro-Beams under Mechanical Shock. *Mechanics Research Communications*, 57, 34-39.